NJC

Accepted Manuscript

This is an *Accepted Manuscript*, which has been through the Royal Society of Chemistry peer review process and has been accepted for publication.

Accepted Manuscripts are published online shortly after acceptance, before technical editing, formatting and proof reading. Using this free service, authors can make their results available to the community, in citable form, before we publish the edited article. We will replace this *Accepted Manuscript* with the edited and formatted *Advance Article* as soon as it is available.

You can find more information about *Accepted Manuscripts* in the Information for Authors.

Please note that technical editing may introduce minor changes to the text and/or graphics, which may alter content. The journal's standard Terms & Conditions and the Ethical guidelines still apply. In no event shall the Royal Society of Chemistry be held responsible for any errors or omissions in this *Accepted Manuscript* or any consequences arising from the use of any information it contains.

ROYAL SOCIETY OF CHEMISTRY

www.rsc.org/njc

New Journal of Chemistry

PAPER

High Activity of Aluminated Bifunctional Mesoporous Silica Nanoparticles for Cumene Hydrocracking and Measurement of Molar Coefficient Absorbance

Mohammad Reza Sazegar[a,b] *, Sugeng Triwahyono[b] , Aishah Abdul Jalil[c], Rino R. Mukti[d], Seyed Mohammad Seyed Mohaghegh[e,f] and Madzlan Aziz[b]

Bifunctional mesoporous silica nanomaterials (MSN) with various Si/Al molar ratios of 7, 10, 20 and 50 in platinum supported (Pt/HAlMSN) were synthesized using sol-gel followed by post-synthesis methods. XRD and nitrogen sorption results confirmed the mesoporous structure with the surface areas of 537–775 m^2g^{-1}. ^{27}Al NMR spectroscopy confirmed aluminium loading with tetrahedral, pentahedral and octahedral structures. Pyridine adsorbed IR results indicated that the aluminium incorporating led to generate strong Brønsted and Lewis acidic sites. Catalytic activity was investigated for cumene hydrocracking in a pulse microcatalytic reactor at the temperature range of 323–573 K which revealed that this activity depends on the number of Lewis and Brønsted sites. High yield of cumene conversion increased from Si/Al of 50 to 10 and decreased in Si/Al of 7 due to the presence of pentahedral Al and/or inactive tetrahedral Al atoms in Pt/HAlMSN-7. High selectivity of α-methylstyrene showed the important role of Lewis acid sites in these bifunctional catalysts. In spite of the coke formation in the Pt/HAlMSN catalysts, the reactivation recovered the activity of catalysts after 100 h of reaction. The molar coefficient absorbances of Pt/HAlMSN were measured using pyridine followed by water adsorption monitored by FTIR.

Received 00th January 2015,
Accepted 00th January 2015

DOI: 10.1039/x0xx00000x

www.rsc.org/

Introduction

Mesoporous silica nanoparticles (MSN) with specific characteristics like large surface area, high pore size and volume, catalysis behavior and adsorption properties open up many potential applications in catalysis, environmental protection and nanostructured materials[1-3]. Aluminium loading into MSN in order to produce active sites results in a decrease of the pore structure as compared with the pure MSN[4]. Protonation of mesoporous materials changes the pore structure as well as undesirable loss of 4-coordinated aluminium structure and appearance of 6-coordinated aluminium structure[5]. Introduction of platinum to the mesoporous silica materials usually combined with metal oxides such as Zr, Ir, Al and Mo oxides[6-8] which increased the catalytic activity. Enhancement in the amount and strength of the acidic sites conducted through the generation of Brønsted acid sites by using protonation process.

Recently, Jana *et al.*[9] synthesized the catalyst of Al-MCM-41 (Mobil Composition of Matter No. 41) with different molar ratios of Si/Al via four different synthesis methods: hydrothermal, grafting, sol-gel and template cation exchange. They showed that the

[a] Dept. of Chemistry, Fac. of Science, North Tehran Branch, Islamic Azad University, Tehran, Iran Tel: +982122262564 E-mail: m_r_sazegar@yahoo.com
[b] Dept. of Chemistry, Fac. of Science, Universiti Teknologi Malaysia, 81310 UTM Johor Bahru, Johor, Malaysia
[c] Institute Hydrogen Economy, Dept. of Chemical Eng., Fac. of Chemical Eng., Universiti Teknologi Malaysia, 81310 UTM Johor Bahru, Johor, Malaysia
[d] Division of Inorganic and Physical Chemistry, Fac. of Mathematics and Natural Sciences, Institut Teknologi Bandung, Jl Ganesha No 10, Bandung, 40132 Indonesia
[e] Dept. of Chemical Engineering and applied chemistry, University of Toronto, Toronto, ON, Canada
[f] Dept. of Polymer Science, Iran Polymer and Petrochemical Institute, Tehran, Iran

See DOI: 10.1039/x0xx00000x

acidity and catalytic activity increased with the increase of Al loaded into the catalyst structure. Al-MCM-41 showed the highest activity in the cracking reaction in comparison with zeolite Y, SBA-15 (Santa Barbara Amoprhous 15) and ZSM-5 (Zeolite Socony Mobil–5) due to the highest acidity of Al-MCM-41[10]. Handjani *et al.*[11] synthesized Pt/Al-SBA-15 catalyst and showed that lower amount of Brønsted acid sites and higher amount of Lewis acid sites had influenced in the activity of catalyst in cumene cracking.

Whereas few studies have been reported the synthesis of Al-containing and platinum supported on mesoporous silicates, this study focused on the synthesis and characterization of protonated AlMSN with platinum supported in the cracking reaction. MSN exhibits low catalytic activity due to the presence of weak Lewis acid sites and the absence of Brønsted acid sites in its framework. Incorporation of aluminium followed by protonation generates the strong Lewis and Brønsted acid sites which lead to increase the catalytic activity. In the present work, the catalyst of Pt/HAlMSN with different Si/Al ratio of 7-50 was synthesized and cumene hydrocracking reaction was investigated in order to evaluate the effect of Al concentration accompany by platinum species over cumene conversion. We reported here the synthesis of MSN by sol-gel method and incorporation of aluminium with different Si/Al ratio of 7, 10, 20 and 50 followed by protonation resulted HAlMSN which was found to enhance the acidity, activity and stability of MSN. Platinum loading of HAlMSN (denoted Pt/HAlMSN) was carried out as much as 0.1 wt% Pt which promoted the active sites for cumene hydrocracking reaction. The physical properties of Pt/HAlMSN were confirmed by nitrogen physisorption, XRD, FTIR, pyridine-FTIR and 29Si and 27Al solid state NMR. The activity of the Pt/HAlMSN catalysts was examined using the cracking of cumene under hydrogen atmosphere. The conversion results revealed that the activity of the catalysts was strongly related to the number of Lewis and Brønsted acid sites. The role of platinum particles, Brønsted and Lewis acid sites in the formation of propene, benzene, toluene and α-methylstyrene in cumene cracking reaction were discussed in details.

Experimental

The preparation method

General procedure of Pt/HAlMSN synthesis

The synthesis of MSN was carried out according to the previous reported procedure[2]. The mesoporous MSN was prepared using 1,2-propanediol (PD) as a co-solvent in sol-gel method. Cetyltrimethylammonium bromide (CTAB, 1.17g) was dissolved in an aqueous solution containing double distilled water (180g) and 1,2-propanediol (PD, 30 mL) in an aqueous ammonia solution (7.2 mL, 25%). After vigorous stirring for approximately 30 min at 323 K, tetraethyl orthosilicate (TEOS, 1.43 mL) and 3-aminopropyl triethoxysilane (APTES, 0.263 mL) were added to the mixture. The resulting mixture was stirred for an additional 2 h at 323 K and allowed to rest for 20 h at the same temperature. The gel composition used in the synthesis of the parent MSN was 1TEOS:0.17APTES:0.5CTAB: $13.5NH_3$:85.2PD:$1042H_2O$.

The sample was collected by centrifugation for 30 min at 20,000 rpm and washed with deionized water and absolute ethanol 3 times. The surfactant was removed by heating MSN (1 g) in an NH_4NO_3 (0.3 g) and ethanol (40 mL) solution at 333 K. The surfactant-free product was collected by centrifugation and dried at 383 K overnight prior to calcination in air at 823 K for 3 h. The acidic sites of the samples were prepared by aluminium grafting on the template-free MSN at 353 K for 10 h followed by centrifugation and dried at 383 K overnight prior to calcination in air at 823 K for 3 h. Sodium aluminate (Sigma-Aldrich) was used as a precursor of aluminium. Al-grafted MSN was denoted as AlMSN. The initial molar ratios of Si/Al were 7, 10, 20 and 50. The AlMSN samples were synthesized by adding MSN (1 g) in an aqueous solution (50 mL) of sodium aluminate (0.154, 0.110, 0.054 and 0.022 g) for Si/Al ratios of 7, 10, 20 and 50, respectively, at 353 K for 10 h followed by centrifugation and dried at 383 K overnight prior to calcination in air at 823 K for 3 h with a heating rate of 1 K min^{-1}. The protonated AlMSN (HAlMSN) sample was synthesized by protonation of AlMSN (1g) using aqueous solution of NH_4NO_3 (2.5g in 50 mL of double distilled water) at 333 K for 16 h followed by removal of solution, drying at 383 K overnight and calcination at 823 K for 3 h in air. The Pt/HAlMSN catalysts were prepared by impregnation of HAlMSN with 0.1 wt% Pt solution followed by calcination in air at 823 K for 3 h. Chloroplatinic acid hydrate ($H_2PtCl_6 \cdot 6H_2O$, Sigma-Aldrich) was applied as a source of platinum.

Catalyst Characterization

The crystallinity of catalysts was measured with a Bruker Advance D8 X-ray powder diffractometer with Cu Kα (λ=1.5418 Å) radiation as the diffracted monochromatic beam at 40 kV and 40 mA. Nitrogen physisorption analysis was conducted on a Quantachrome Autosorb-1 at 77 K. Before the measurement, the sample was evacuated at 573 K for 3 h.

The elemental analysis of the catalysts were determined by Bruker S4 Explorer X-ray fluorescence spectroscopy (XRF) using Rh as anode target material operated at 20 mA and 50 kV. XRF analysis showed that the Si/Al ratio of the Pt/HAlMSN frameworks were 5.6, 9.0, 18.9 and 48.7 for S_7, S_{10}, S_{20} and S_{50}, respectively.

Fourier Transform Infra-Red (FTIR) measurements were carried out using Agilent Carry 640 FTIR Spectrometer. The catalyst was prepared as a self-supported wafer and activated under H_2 stream (F_{H2}=100 mL/min) at 623 K for 3 h, followed by vacuum at 623 K for 1 h[2,7]. To determine the acidity of the catalysts, the activated samples were exposed to 2 Torr pyridine at 423 K for 30 min, followed by evacuation at 473 K for 1 h to remove physisorbed pyridine on the samples. In order to study the effect of activation temperature, the Pt/HAlMSN was activated at four different temperatures of 473, 523, 573 and 623 K. All spectra were recorded at room temperature. All spectra were normalized using the overtone and combination vibrations of the lattice of MSN between 2200 and 1300 cm^{-1} after activation, particularly the lattice peaks at 1855 cm^{-1} [2]. The number of Brønsted and Lewis acid sites was calculated using the integrated molar adsorption coefficient values.

The measurement of molar absorption coefficients of the catalysts was carried out by using IR spectroscopy. In this method the infrared experiments were carried out using 50 mg of sample pressed into a 15 mm diameter disk. Spectra were recorded after the initial evacuation of the sample at 673 K for 1 h and then after exposure to 1 Torr pyridine and evacuation at 423 K for 15 min, followed by outgassing at the same temperature. The IR spectrum was recorded at room temperature. Then, the amount of 5 Torr of water was introduced to the sample at 423 K for 2 h. After this period, FTIR spectra was recorded at room temperature with the integrated areas of the bands at 1455 and 1545 cm^{-1} due to the 19b ring vibrations of pyridine adsorbed at Lewis and Brønsted sites, respectively. The molar absorption coefficient and the value of Brønsted and Lewis acid sites were measured by exposed 1 Torr of pyridine at 423 K for 15 min and outgassing at the same temperature, followed by adsorption of 1 Torr excess pyridine at 423 K for 20 min without followed by outgassing. Then, the IR spectrum was recorded at room temperature.

^{29}Si MAS NMR spectra were recorded on a Bruker Avance 400 MHz spectrometer at 79.49 MHz with 18 s recycle delays and spun at 7 kHz to determine the chemical status of the Si in the silicate framework of catalysts. ^{27}Al MAS NMR spectra were recorded at 104.3 MHz with 0.3 s recycle delays and spun at 7 kHz to determine the chemical status of aluminium in the silicate framework of catalysts[12].

Catalytic Activity

Hydrocracking of cumene was carried out under atmospheric pressure in a microcatalytic pulse reactor coupled with an online 6090N Agilent FID/TCD Gas Chromatograph equipped with a VZ-7 packed column. About 0.2 g of the catalyst was placed in an OD 10 mm quartz glass reactor and subjected to air (F_{Air}=100 mL/min) stream for 1 h and hydrogen (F_{H2}=100 mL/min) stream for 4 h at 623 K[2]. A dose of cumene (36 µmol) was injected over the catalyst at the reaction temperature and the products were trapped at 77 K before flushing out to the gas chromatograph. In order to find the appropriate condition of cumene cracking, the reaction was done at the different temperature range of 323- 523 K.

The cumene conversion (X_{cumene}) and selectivity of the products (S_i) were calculated according to Eq.(1) and Eq.(2) , respectively:

$$X_{Cumene}(\%) = \frac{C_{in}-C_{out}}{C_{in}} \times 100\% \qquad (1)$$

$$S_i(\%) = \frac{C_i}{(\sum C_i)-C_{cumene}} \times 100\% \qquad (2)$$

Where C_{in}, C_{out}, C_i and C_{cumene} are mole number of cumene in the inlet, outlet, particular compound and residual cumene, respectively, which calculated based on the Scott hydrocarbon calibration standard gas (Air Liquid America Specially Gases LLC). The *i* is the number of particular carbon.

Results and Discussion

Preparation of catalyst

The parent MSN was synthesized through sol-gel technique and the Pt/HAlMSN samples were prepared by aluminium loading of MSN followed by introduction of platinum. XRD patterns of the Pt/HAlMSN samples with Si/Al molar ratios of 50 to 7 are given in Fig.1. An intense diffraction peak (100) at low angle degree between 2θ=2.28-2.40° and two small signals (110, 200) at 2θ = 4-5° were observed. The peaks were confirmed the presence of two-dimensional hexagonal (*p*6mm) structure with d_{100}-spacing of approximately 3.6 nm. Incorporation of aluminium into MSN reduced the order of hexagonal mesoporous structures significantly[1]. The shift in peak position from 2.28° to 2.40° may be due to the substitution of Si atoms with larger atomic radius of Al atoms which led to enhance in the interplanar spacing of MSN.

Table 1 showed the physical characteristics of Pt/HAlMSN catalysts with ratio of 50 to 7. The surface areas were shown 775, 620, 537 and 361 m^2g^{-1} for Pt/HAlMSN-50 to Pt/HAlMSN-7, respectively, which indicated to the loading of aluminium on the catalyst surfaces. Decrease in the surface area exhibited the direct relationship with Al content which showed the change in the pore size distribution in the catalysts which probably due to the presence of extra-framework aluminium (EFAl) inside the pore[13]. ^{27}Al MAS NMR spectra confirmed the presence of octahedral Al atom in the Pt/HAlMSN catalysts structure. The grafting of MSN with sodium aluminate has plugged the pores of MSN with diameter around 3.5-4 nm (Fig. 2B). The plugging of the MSN increased with increasing the Al loading which led to decrease the pore size and volume (Table 1). The aluminium species placed inside and/or on the mouth of the pores[2]. Increase in the Al loading decreased the pore volume from 0.40 to 0.15 cm^3g^{-1} and the pore size from 3.77 to 3.64 nm. The wall-thickness increased with Al incorporation from 0.47 to 0.56 nm while, it decreased to 0.40 nm in Pt/HAlMSN-7. This decrease indicated that aluminium and residual sodium placed inside and outside of the pores in the Al-rich sample with Si/Al ratio of 7.

Similar results had been reported on aluminium immobilized mesoporous of MCM-41 by Chen *et al.*[14]. The introduction of aluminium to MCM-41 decreased the surface area from 1151 to 336 m^2g^{-1} for Al-MCM-41 with Si/Al ratios of 15.3 to 1.9, respectively.

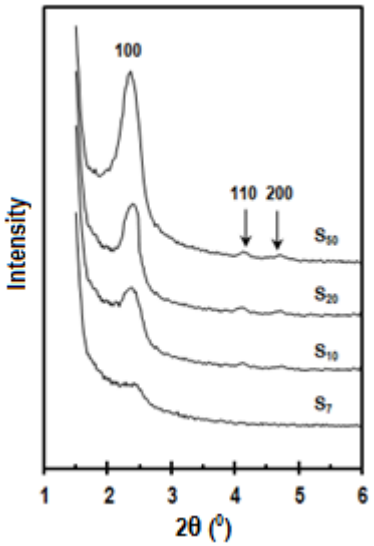

Fig. 1 XRD patterns of the Pt/HAlMSN catalysts with the Si/Al molar ratio of 7-50

In addition, the presence of platinum in Pt/HAlMSN was investigated by using FESEM-EDX images and XRF analysis (supplementary data, appendices 1 and 2).

Fig. 2A-B exhibit nitrogen adsorption-desorption isotherms and corresponding pore size distribution of Pt/HAlMSN catalysts which was calculated by NLDFT method. The nitrogen sorption isotherms pattern of the samples exhibit Type IV with H1-type hysteresis loops for all samples which attributed to the mesoporous silica with uniform cylindrical pores (Fig. 2A).

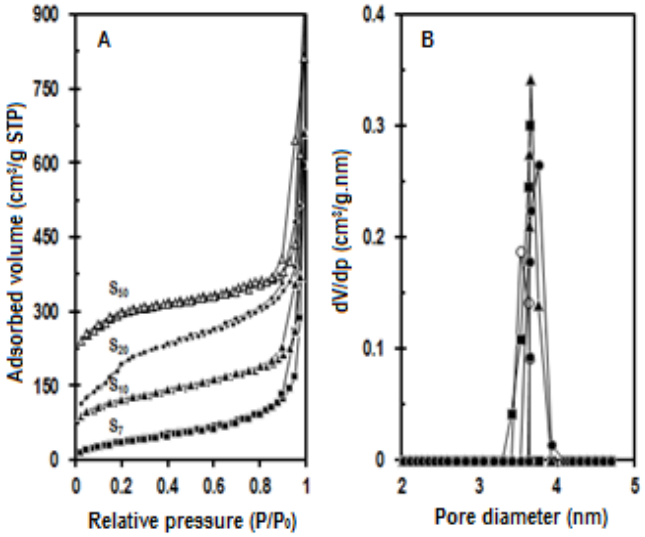

Fig. 2 (A) Nitrogen adsorption - desorption isotherms and (B) pore size distribution for Pt/HAlMSN with Si/Al of 7 (○), 10 (■), 20 (▲) and 50 (●)

Table 1 Physical characteristics of the Pt/HAlMSN catalysts

Catalyst	d_{100} (*nm*)	a_0 (*nm*)	*S* (m^2/g)	V_p (cm^3/g)	*W* (*nm*)	*t* (*nm*)	*Si/Al (exp.)*	*Si/Al (XRF anal.)*
Pt/HAlMSN-7	3.50	4.04	361	0.15	3.64	0.40	7	5.6
Pt/HAlMSN-10	3.65	4.21	537	0.18	3.65	0.56	10	9.0
Pt/HAlMSN-20	3.59	4.15	620	0.29	3.67	0.48	20	18.9
Pt/HAlMSN-50	3.67	4.24	775	0.40	3.77	0.47	50	48.9

d_{100}, *d*-value 100 reflections; a_0, pore center distance is equal to $2d_{100}/\sqrt{3}$; *S*, BET surface area (m^2/g) obtained from N_2 adsorption; V_p, total pore volume (cm^3/g), *W*, pore size (nm) obtained from BJH method, t, pore wall thickness is equal to a_0-*W*; *Si/Al (exp.)*, experimental Si/Al molar ratio; *Si/Al (XRF anal.)*, Si/Al molar ratio analysed by XRF.

The isotherms of catalysts show an inflection characteristic of capillary condensation at relative pressure of $0.1< P/P_0 <0.3$, which displays characteristic of porous structures with small and uniform mesopore[15]. A significant increase at higher relative pressure in the range of 0.8-1.0 indicates the presence of a textural porosity which is owing to the less ordered mesoporous structure due to the loading of Al into the pure mesopore silica materials. Increase in the Al loading altered slightly the properties of sample. The presence of Al species plugged inside the microporous of the catalysts which led to decreases the inflection at $P/P_0<0.2$ and decreases the intensity of pore size distribution.

In agreement with the results of nitrogen physisorption and XRD patterns, Subhan and cooperators[16] loaded Al over MCM-41 by post-synthesis method in the various Si/Al molar ratio ranges of 30 and 50. The XRD patterns showed an ordered hexagonal structure for the Al-MCM-41 samples. The BET results revealed a decrease in the surface area from 925 to 556 m^2g^{-1} and reduce the pore volume from 0.60 to 0.49 cm^3g^{-1} and no significant variation in the pore size distribution was observed.

Fig. 3 shows the ^{29}Si MAS NMR and ^{27}Al MAS NMR spectra of the Pt/HAlMSN catalysts. The chemical shift of ^{29}Si NMR in aluminosilicates depends on the number of Al atoms in the coordination with Si atoms and the peaks observe broader with increasing Al concentration. The mesoporous silica materials consist of a significant proportion of silanol groups, which decreases with alumination process. Typically, the chemical shift is about -110 ppm for $Si(OSi)_4$ units[17]. The corresponding signals overlap with those of Q^2 and Q^3 species, which makes difficult to estimate the extent of aluminium from ^{29}Si NMR spectra. ^{29}Si NMR spectra of the series of exchanged samples are clearly shifted from -104 ppm for Pt/HAlMSN-50 to -97 ppm for Pt/HAlMSN-7. This confirms that the fraction of Si(OAl) species increased due to substitution of more Al into the mesoporous silica walls which is ascribed to AlO-$Si(OSi)_3$ and/or HO-$Si(OSi)_3$, $(AlO)_2$-$Si(OSi)_2$ and/or $(HO)_2$-$Si(OSi)_2$ sites. This result is in excellent agreement with the evolution of tetrahedral Al structure[17].

In ^{27}Al MAS NMR spectra, signal at 53 ppm described the presence of tetrahedrally (T_d) coordinated aluminium framework and a small peak at 28 ppm depicted to pentahedral Al species and 0 ppm was assigned to octahedrally (O_h) coordinated aluminium non-framework[10]. This indicates that the high aluminium incorporation causes the ''flaking-off'' of Al atoms from tetrahedral sites in the mesoporous walls to octahedral and pentahedral sites. The pentahedrally coordinated Al is indicative of the defects of grafted Al phase[18]. Pt/HAlMSN-7 showed 4-, 5- and 6-coordinated Al structures while the other samples exhibited 4- and 5-coordination. Consequently, generation of non-acidic Al structure in the Al-rich sample is probably due to the presence of paired framework Al atoms and five-coordinated aluminium located at the interface between the tetrahedral aluminosilicate framework and the octahedral alumina phase[19].

Similarly, Bhange *et al.*[20] reported the modification SBA-15 by loading of the various amounts of aluminium which led to observe of octahedrally, pentahedrally and tetrahedrally coordinated Al structures at 1, 30 and 52-54 ppm, respectively.

FTIR spectra of the Pt/HAlMSN catalysts at the range of 3800-3500 cm^{-1} are shown in Fig. 4A.

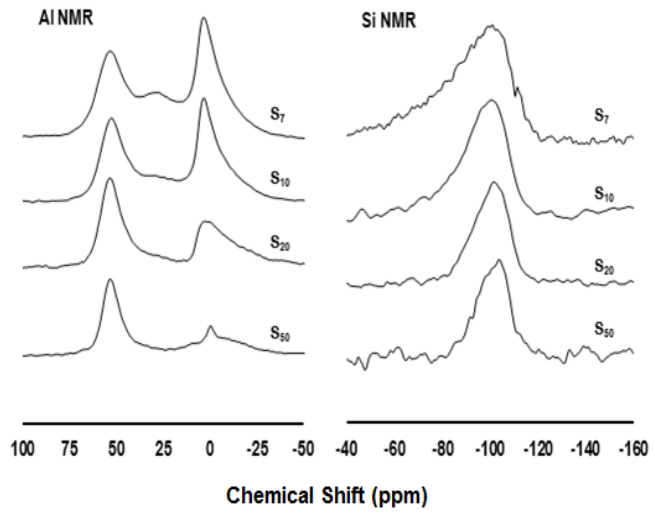

Fig. 3 ^{29}Si NMR and ^{27}Al MAS NMR of the Pt/HAlMSN catalysts with Si/Al ratio of 7-50

The sharp band at 3740 cm-1 is assigned to the non-acidic isolated silanol hydroxyl groups (Si-OH) observed on the external surface of mesoporous catalysts[21]. Decrease in the H-bonds of hydroxyl groups is an evidence for the increase substitution of Al atoms into the framework. These silanol groups were observed inside the channels and were connected with structural imperfections or local defects[21].

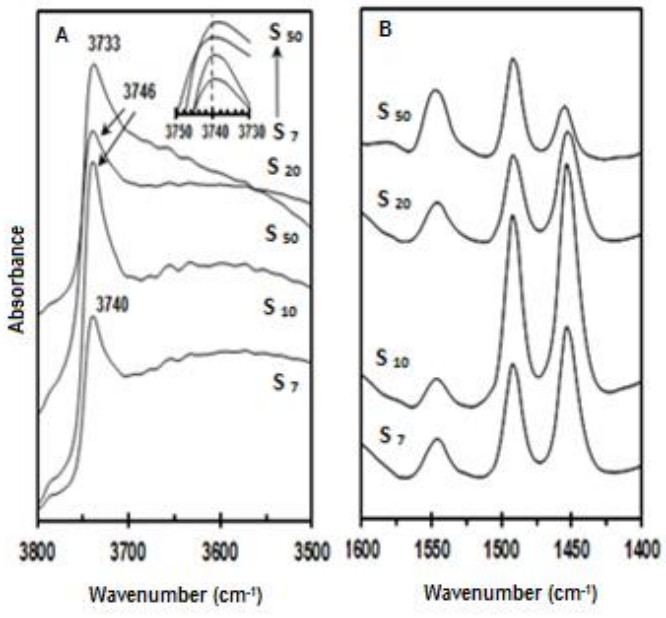

Fig. 4 (A) FTIR spectra of the Pt/HAlMSN catalysts with Si/Al ratio of 7-50 for hydroxyl groups stretching region at 3500 – 3800 cm^{-1}; (B) Pyridine adsorbed FTIR spectra of Pt/HAlMSN with Si/Al ratio of 7-50. Pyridine was adsorbed at 423 K for 30 min, followed by outgassing at 473 K for 1 h

IR spectra of the Pt/HAlMSN catalysts also showed the bridge hydroxyl group of Si-OH-Al at 3552 and 3637 cm^{-1} which is assign to the framework Al atom. The broad band at 3660 cm^{-1} is assigned to the presence of Si-OH-Al…..Al structure and show the interaction of OH group with extra-framework Al which is assign to the presence of octahedral Al atom[22].

The peak observed at 3520 cm^{-1} illustrated the hydrogen-bonded internal Si-OH groups which decreased with more aluminium grafting. The peak at 3580 cm^{-1} is assigned to H-bonded OH and described the weak acidic property[22].

Brønsted and Lewis acidity in the Pt/HAlMSN solid catalysts

The effect of Si/Al ratio and temperature was observed in the acidity of the catalysts. The number of acid sites was altered by the aluminium concentration. The number of Lewis acid sites increased and the number of Brønsted acid sites decreased with enhancing the Al content and the temperature. Increase the temperature enhanced the removal of hydrogen from the Brønsted acid sites which resulted diminish this sites and enhancing Lewis acidity.

Fig. 4B shows the acidity of Pt/HAlMSN which adsorbed pyridine at room temperature, followed by evacuation at 673 K. The pyridine-IR spectrum at 423 K shows the Lewis and Brønsted acid sites at 1455 and 1545 cm^{-1}, respectively. Increase in Lewis acid sites indicate to the increase in Al concentration due to the replacement of Al species with Si atoms. Tetrahedrally coordinated Al^{3+} ions was responsible of Lewis acid formed through the isomorphous substitution of Si^{4+} lattice sites by Al^{3+} ions, leading to generate of an aluminosilicate phase[23]. The relationship between the framework Al concentration and acid strength may be explained by the presence of Al atoms in the second neighbor which can be supposed to have increased Lewis acidity[18]. The presence of tetrahedral and octahedral Al structures in these catalysts which are responsible for the Lewis and Brønsted acid sites, respectively, were confirmed by ^{27}Al MAS NMR and pyridine adsorbed FTIR spectra.

Wang *et al.*[17] reported the synthesis a low-silica AlMCM-41 with Si/Al=1.25 and studied the gradual collapse in their frameworks during dealumination process. The fraction of tetrahedral Al in the solid

decreased with level of dealumination. The presence of platinum on these catalysts did not significantly modify on the intensity of Brønsted and Lewis bands. The acidic properties of platinum loaded nanoparticles have not directly influenced in the hydrocracking activity[24]. The Brønsted acid strength decreased and Lewis acidity increased while Al content increased.

Fig. 5A-D show IR spectra of the Pt/HAlMSN samples which were activated at 473, 523, 573 and 623 K for 3 h, then pyridine was adsorbed at 423 K for 30 min, followed by outgassing at 473K. Fig. 5E-F illustrated variation of the intensity of Lewis and Brønsted acid sites determined by pyridine desorption. The number of Lewis acid sites increased (Fig. 5E) while Brønsted acid sites decreased (Fig. 5F) with raising the temperature. Pt/HAlMSN-7 showed less Lewis acidity than Pt/HAlMSN-10 due to the presence of inactive framework Al structure in this catalyst. Decrease the Brønsted acid sites indicate the removal of hydrogen with temperature and subsequently increased the number of Lewis acid sites.

Measurement of molar absorption coefficients of the Pt/HAlMSN catalysts

The activity of the catalysts is related to the ratio of Brønsted acid sites to Lewis acid sites ([B]/[L])[25]. Using pyridine followed by water adsorption monitored by infrared spectroscopic techniques is a method to measure the Brønsted and Lewis acid sites strength[25].

Water is absorbed on Lewis acid sites selectively and formed hydroxyl group as Brønsted acid sites on surface of the sample. This method change all the physically pyridine adsorbed on Lewis aid sites to chemically pyridinium ion adsorbed on Brønsted acid sites[25].

The molar absorption coefficient of pyridinium ion on Brønsted acid sites at 1545 cm^{-1} (ε_{B1545}), the molar absorption coefficient of pyridinium ion on Brønsted acid sites and pyridine on Lewis acid sites at 1490 cm^{-1} ($\varepsilon_{B1490,}$ ε_{L1490}) were calculated. If [B] indicated to the amount of pyridinium ion bind on Brønsted acid sites and [L] assigned to the amount of pyridine bind on Lewis acid site, the ratio of [B]/[L] can be expressed as :

$$[B]/[L] = A_{1545}/(A'_{1545} - A_{1545}) \quad (3)$$

Where, A_{1545} and A'_{1545} were the intensities of the bands at 1545 cm^{-1} before and after adsorption of water, respectively. The molar absorption coefficient of pyridinium ion on Brønsted acid sites at 1545 and 1490 cm^{-1} and pyridine on Lewis acid sites at 1490 cm^{-1} were denoted as $\varepsilon_{1545,}$ ε_{B1490} and ε_{L1490} were as follows:

$$A_{1545} = \varepsilon_{1545}\,[B] \quad (4)$$

$$A_{1490} = \varepsilon_{B1490}\,[B] + \varepsilon_{L1490}\,[L] \quad (5)$$

The ratio of molar absorption coefficient of pyridinium ion on the band at 1490 to 1545 cm^{-1} will be:

$$\varepsilon_{B1490} / \varepsilon_{1545} = A'_{1490}/A'_{1545} \quad (6)$$

$$\varepsilon_{B1490}\,[B] = (\varepsilon_{B1490} / \varepsilon_{1545})\, A_{1545} \quad (7)$$

From the Eq.(4), (5) and (7), ε_{B1490} [B] and ε_{L1490} [L] can be expressed:

$$\varepsilon_{B1490}\,[B] / \varepsilon_{L1490}\,[L] = (\varepsilon_{B1490} / \varepsilon_{L1490})\,([B] / [L]) \quad (8)$$

$$\varepsilon_{B1490} / \varepsilon_{L1490} = (A'_{1490} / A'_{1545})\,(A'_{1545}-A_{1545}) / \{A_{1490}-(A'_{1490}/A'_{1545})\, A_{1545}\} \quad (9)$$

If X_B and X_L were attributed to pyridine adsorbed on Brønsted and Lewis acid sites respectively, the intensities of the bans at 1490 and 1545 cm^{-1} were obtained as follows:

$$A_{1490} = \varepsilon_{B1490}\, X_B + \varepsilon_{L1490}\, X_L \quad (10)$$

$$A_{1545} = \varepsilon_{1545}\, X_B \quad (11)$$

The intensities of the bands at 1490 and 1545 cm^{-1} were measured as:

$$A'_{1490} = \varepsilon_{B1490}\,(X_B + X'_B) + \varepsilon_{L1490}\,(X_L + X'_L) \quad (12)$$

$$A'_{1545} = \varepsilon_{1545}\,(X_B + X'_B) \quad (13)$$

From the Eq. (10) to Eq. (13), ε_{B1490} / ε_{L1490} and ε_{B1490} / ε_{1545} and molar absorption coefficient of ε_{B1490}, ε_{L1490}, ε_{1545} can be calculated. The molar absorption coefficient units, ε were measured by using Beer-Lambert law equation:

$$A = (\varepsilon \times n)/S \quad (14)$$

Where *A* (cm^{-1}), ε (cm μmol^{-1}), n (mole) and *S* (cm^2g^{-1}) assigned respectively the absorbance, the molar absorption coefficient, amount of pyridine adsorbed and the surface of the pressed disk. Calculated molar absorption coefficients for Brønsted and Lewis acid sites in the Pt/HAlMSN catalysts at 1490 and 1545 cm^{-1} and some reported molar coefficient absorbance for

different solid catalysts were shown in Table 2. These studies have been reported the molar coefficient absorbance using a regression analysis of pyridine adsorbed FTIR at 423 K with different Si/Al solid catalysts which they are in good agreement with our results. The calculated values for the pyridine ion (Brønsted sites with corresponding band at 1545 cm^{-1}) varied within the range 0.56–2.2 cm μmol^{-1} and For Lewis sites the average values of ε were 1.44 and 2.22 cm μmol^{-1} [26-30].

Influence of the Si/Al molar ratio and platinum on cumene conversion and selectivity

The influence of Si/Al molar ratio on the cumene hydrocracking over Pt/HAlMSN at the region of 323-523 K was shown in Fig. 6A. The cumene hydrocracking enhanced with increasing the temperature which described that the catalytic activity directly depends on the temperature and Al concentration factors. Increase the Al content increased the catalytic activity through enhance of the catalyst acidity. The bifunctional catalysts of Pt/HAlMSN showed high activity of 84, 88, 97 and 94% for Si/Al ratio of 50-7, respectively, at 523 K. Generally, the presence of platinum in the heterogeneous catalyst promotes the conversion of cumene cracking[31]. According to the published reports, at 523 K, the cumene cracking over the monofunctional catalyst of Al-MCM-41 (Si/Al=20)[32] and Pt-supported MCM-41[33] were 13.5 and 25.1%, respectively, while the bifunctional catalyst of Pt/HAlMSN represented 88% cumene conversion.

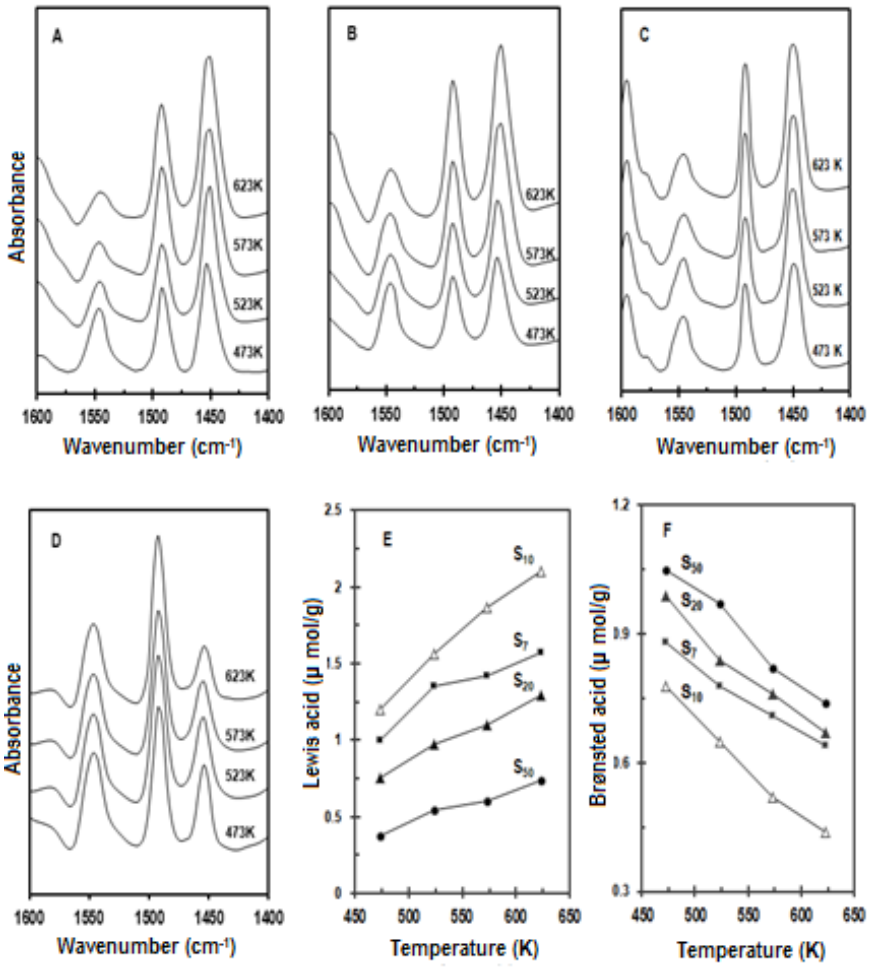

Fig. 5 IR spectrum of Pt/HAlMSN with Si/Al ratio of 7 (A), 10 (B), 20 (C) and 50 (D) which were activated at 473, 523, 573 and 623 K for 3 h, then pyridine were adsorbed at 423 K for 30 min, followed by outgassing at 473K; Variations of the absorbance of IR acid sites (Lewis (E) and Brønsted (F)) with the activated temperatures. Samples were activated at 473, 523, 573 and 623 K for 3 h. Pyridine was adsorbed at 423 K for 30 min, followed by outgassing at 473 K

According to the previous study[2], the cumene conversion over the monofunctional catalyst of HAlMSN (Si/AL=20) showed 55%, while this conversion was 88% for Pt/HAlMSN (Si/Al=20) at 523 K. Therefore, the presence of Pt species plays a significant role in the promoting of cumene conversion[34].

Table 2 The molar absorption coefficients for absorption bands at 1550-1545 cm^{-1} (Brønsted sites, ε_B), 1455-1450 cm^{-1} (Lewis sites, ε_L) and the amount of Brønsted and Lewis acid sites in this study and reported in the literatures

Catalyst	ε_B*	ε_L*	[B]/[L]	Ref.
Pt/HAlMSN-7	1.26	2.08	0.34	This study
Pt/HAlMSN-10	1.49	1.57	0.40	This study
Pt/HAlMSN-20	1.03	1.40	1.12	This study
Pt/HAlMSN-50	1.15	2.17	0.35	This study
Silica-alumina	0.56	1.44	-	26
SiO2, Al2O3	1.80-2.20	-	-	27
Zeolite, ASA	1.67	2.22	-	28
Si-Zr (0.2 in-situ)	0.77	2.08	-	30
Si-Zr (mol%9)	1.32	1.49	-	30
Si-Zr (mol%20)	1.16	1.58	-	30

* IR absorption coefficient (cm μmol^{-1})

The results showed that the catalytic activity of these samples influenced by the presence of the acid sites accompany with Pt species. The platinum sites protect the neighbouring acid sites from deactivation within a determine radius, through the hydrogen spillover process[24]. Hydrogen molecules were adsorbed on Pt sites of the catalysts and generated hydrogen atoms which spillover onto the surface of Pt/HAlMSN and undergo surface diffusion. The hydrogen reaches a Lewis acid center and donates an electron to form H^+ which is stabilized on oxygen atom near the Lewis acid sites. The Lewis acid site traps an electron which then reacts with the second spillover hydrogen to form an H^- bond with a Lewis acid site[34].

Fig. 6A also shows the influence of temperature on cumene conversion and selectivity over the Pt/HAlMSN catalysts. The conversion of cumene reaction increased with enhancing the temperature from 323 to 523 K in a relatively regular trend. The maximum conversion of 84, 88, 97 and 94% was observed at 523 K over Pt/HAlMSN with ratios of 50-7, respectively. The results showed that the generation of pentahedrally Al structure in Pt/HAlMSN-7 decreased the activity of this catalyst in comparison with Pt/HAlMSN-10.

The major products of cumene cracking over Pt/HAlMSN were composed of propene, benzene, toluene and α-methylstyrene. The high activity of cumene conversion was due to the presence of molecular hydrogen and strong Lewis acid sites in which the strong Lewis acid sites acts as active site for the formation of protonic acid sites. The protonic acid sites were responsible of the production of propene, benzene and toluene via dealkylation process, while the strong Lewis acid sites enhanced the dehydrogenation process and produced α-methylstyrene[35,36]. The presence of platinum accelerated the cracking of cumene reaction.

In agreement with obtained results, Corma *et al.* stated that the Brønsted acid sites in the cracking of cumene are responsible for the generation of carbenium ion which lead to form propene and benzene[37]. While the presence of the strong Lewis acid sites accelerates the hydride transfer which enhance the formation of α-methylstyrene. Bradely and Kydd studied the cracking reaction of *iso*-propyl benzene with an alumina supported gallium catalyst to produce propene and α-methylstyrene through solid catalyzed dehydrogenation and cracking reactions[35]. Cumene dehydrogenation has also been explored over complex-derived Cr- and Fe–Cr-pillared clays in which the products of benzene and propene was produced at low temperature, and α-methylstyrene was observed at higher temperatures[36].

Fig. 6B-D shows the selectivity of α-methylstyrene, propene and benzene as the selected products of cumene conversion at the range of 323-573 K in a microcatalytic pulse reactor under hydrogen carrier gas. In all catalysts, α-methylstyrene was produced due to the predominant effect of Lewis acid sites during dehydrogenation mechanism which reduced with increasing the temperature. The selectivity of α-methylstyrene is 75, 65, 45 and 42%, respectively, at 473 K, for the samples with Si/Al ratio of 20, 50, 7 and 10. The order of α-methylstyrene formation is due to the number of Lewis acid sites in the catalysts. The amount of α-methylstyrene decreased with the increase of the temperature. Therefore, α-methylstyrene selectivity decreased with reducing the number of Lewis acid sites in accordance with Si/Al ratio of 20 > 50 > 7 > 10. The amounts of propene and benzene gradually increased with the temperature which confirmed the role of protonic acid sites.

The mechanisms of cumene cracking were proposed in terms of the generated ions due to the operation of Lewis and Brønsted acid sites. The formation of α-

methylstyrene in cumene hydrocracking is attributed to Lewis acidity, according to dehydrogenation mechanism (scheme 1). This mechanism of cumene conversion involves several modes: firstly, Lewis acid attaches to the aromatic ring and generates a cation site; secondly, the C-H bond of methyl group cleavage and then hydrogen shifts from methine group of propyl to the cation site in order to neutralize the positive charge; finally, Lewis acid and hydrogen molecule separate and then forms α-methylstyrene in which the separated Lewis acid will be applied for a new attach to the aromatic carbon[38].

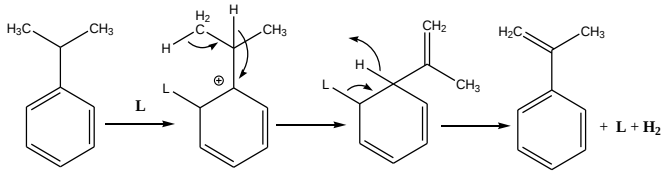

Scheme 1 Mechanism of α-methylstyrene formation (dehydrogenation process) on Lewis acid sites of the Pt/HAlMSN catalysts[38]

Another mechanism is based on the generation of carbenium ion in cumene conversion reaction which gives propene and benzene attributed to the interaction of protonic acid site generated from molecular hydrogen. The mechanism of dealkylation is ascribed to the operation of the Brønsted acid sites on the surface of catalyst (scheme 2). This mechanism of cumene cracking includes the following steps: (1) protonation at the aromatic carbon in which isopropyl group is attached, (2) generation of propyl cation and benzene compound and (3) deprotonation of propyl cation to produce propene and proton which will be applied for the protonation at the aromatic carbon[39].

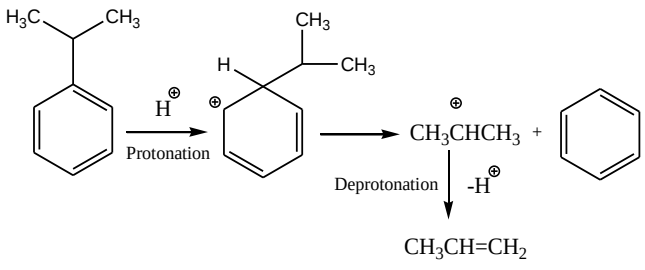

Scheme 2 Mechanism of propene and benzene formation (dealkylation process) on the Brønsted acid sites of the Pt/HAlMSN catalysts[39]

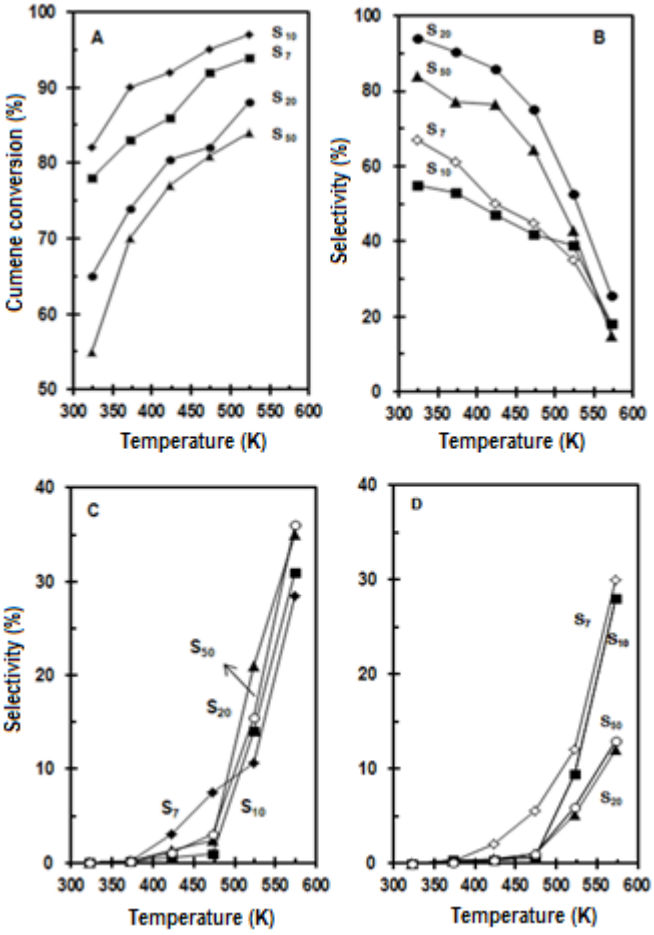

Fig. 6 (A) Relationship between the Si/Al molar ratio and cumene conversion at the region of 323, 373, 423, 473 and 523 K; The selectivity of (B) α-methylstyrene, (C) propene and (D) benzene formation over the Pt/HAlMSN catalysts

Influence of temperature on cumene conversion and products selectivity

Fig. 6 also shows the influence of temperature on cumene conversion and selectivity over the Pt/HAlMSN catalysts. The conversion of cumene reaction increased with enhancing the temperature from 323 to 523 K in a relatively regular trend. Increase of the catalytic activity with enhancing the temperature over these bifunctional catalysts is an evidence to carry out of the spillover phenomenon due to the presence of platinum species[7]. In this process the molecules of hydrogen dissociate on Pt particles and react with cumene molecules on the surface acid sites and application of higher temperature increases the spillover process on the surface active sites. Using higher temperature increases the spillover process on the surface active

sites[7]. This indicates to the effect of Al species as a co-promoting agent for active Pt sites. The cumene conversion trend is similar to the operation of Lewis acid sites.

The role of acid sites on cumene conversion

The role of acidic sites was strongly evidenced by the activity–acidic sites relationship which shown in Fig. 7. The ratio of the cumene conversion to the concentration of Lewis acid sites gradually changed in the temperature range of 473–573 K, while the ratio of the concentration to the Brønsted acid sites exhibited more altered. In fact, the slope of the lines related to the Brønsted acid sites is more in comparison with that of the Lewis acid site.

This result indicated that the cumene conversion is more correlated with the concentration of Lewis acid sites in which the Lewis acid sites have important roles in the stabilization of the formed protons and facilitating the dehydrogenation process. Thus, according to the obtained results, the most activity of Pt/HAlMSN is due to the number of Lewis acid sites. On the other hand, the presence of permanent Brønsted acid cannot be directly associated with the cumene conversion activity over Pt/HAlMSN[2]. In fact, the conversion was low for the cumene conversion in the absence of molecular hydrogen.

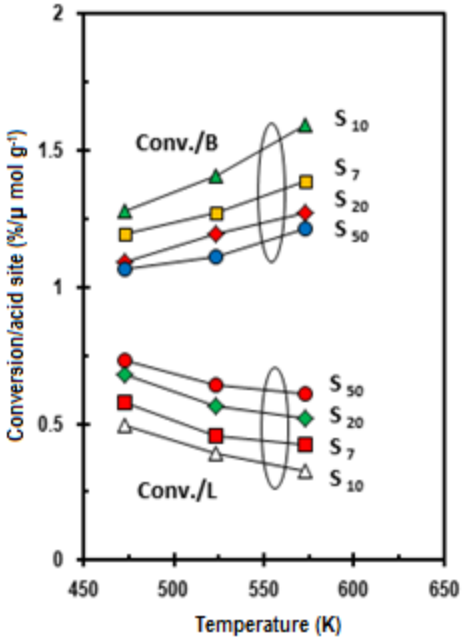

Fig. 7 The relation between cumene conversions with the number of acidic sites at 473–573 K

Table 3 shows the comparison study of cumene conversion over several types of solid catalysts such as Pt/HAlMSN, HAlMSN[2], commercial γ-Al_2O_3[2], Al-MCM-41[40], Al-SBA-20[9], HMFI-SBA-15[41], Pt/ SiO_2 mixed with H-β[42], MOR[43], Pt/Al-SBA-15[11] and Pt/Al_2O_3-MCM-41[33]. The results showed that the activity of Pt/HAlMSN for cumene conversion is higher than the other catalysts at the same or closed temperature. The reason probably is due to the presence of extra-framework aluminium which generates strong Lewis acid sites[2] and the presence of platinum species which provides more interaction between active sites and reactant or hydrogen carrier gas through the spillover phenomenon.

Table 3 The activity of cumene conversion over Pt/HAlMSN and the other type of solid acid catalysts in the presence of hydrogen gas.

Catalyst	Cumene conv. (%)	Temp. (K)	Ref.
Pt/HAlMSN-50	84	523	This study
Pt/HAlMSN-20	88	523	This study
Pt/HAlMSN-10	97	523	This study
Pt/HAlMSN-7	94	523	This study
HAlMSN-20	55	523	2
Commercial γ-Al_2O_3	Trace	523	2
Al-SBA-15(Si/Al=20)	17.1	523	9
20-Al-MCM-41	13.5	573	40
5-Al-MCM-41	3.4	673	9
HMFI-SBA-15	15	573	41
Pt/SiO_2 + H-Beta	30	503	42
FSM-Al-7.8	26.7	673	43
Pt/Al-SBA-15	Trace	573	11
Pt/Al_2O_3-MCM-41	31.2	523	33

Stability Testing

The stability tests of all catalysts are shown in Fig. 8, where the cumene conversion (%) is plotted as a function of the time (h). The conversions of cumene were 94, 97, 88 and 84 % for Pt/HAlMSN with Si/Al ratios of 7 to 50 at 523 K, respectively. The activity of these catalysts was studied with more than 100 h[40]. The activities were slightly decreased with the reaction time for more than 100 h. After stability testing, all spent catalysts were subjected to XRD and FTIR in order to study their properties.

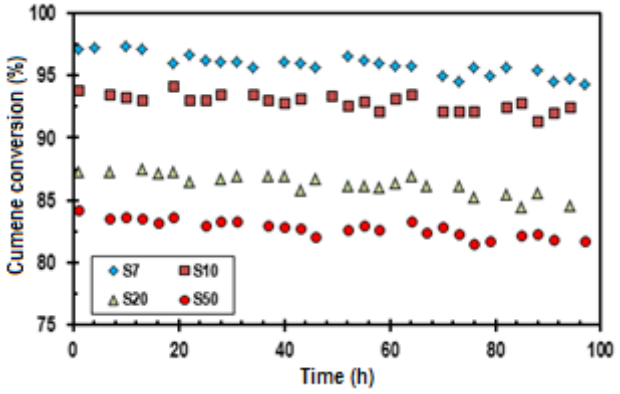

Fig. 8 Stability test of the Pt/HAlMSN catalysts at reaction temperature of 523 K

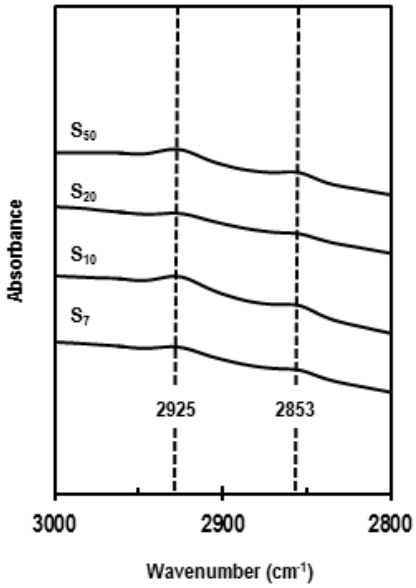

Fig. 9 FTIR spectra of the used Pt/HAlMSN; Cumene conversion was done at 523 K in the presence of hydrogen stream

XRD results (not shown) indicated that there is no significant change after the reaction; however, coke deposits were observed on the used catalysts. The strong distinctive band corresponds to the vibration of C=C observed at 1645 cm^{-1}, which may be related to the presence of olefinic species[2]. In addition, two weak bands observed at 2850 and 2925 cm^{-1} confirmed the presence of the C-H stretching vibration, which is related to the aliphatic hydrocarbons (Fig. 9).

These results show that decrease in activity may be due to the undesirable carbon deposition on the pores of catalysts during the cumene conversion. The coke formation gave a little effect on the activity of the catalysts. This probably indicated that the high activity may be due to the large amount of active surface area and pore size which were still remained after 100 h of reaction.

Conclusion

The effects of Si/Al molar ratio on the properties and activity of Pt/HAlMSN in cumene cracking were studied by using different Si/Al molar ratio of 7, 10, 20 and 50. XRD and N_2 physisorption results indicated that the increase in Si/Al ratio enhanced the percentage crystallinity and hexagonal ordered structures of the catalysts. This led to reduce of specific surface area from 775 m^2g^{-1} for Pt/HAlMSN with Si/Al ratio of 50 to 361 m^2g^{-1} Pt/HAlMSN with Si/Al ratio of 7. The pore volume also decreased from 0.40 to 0.15 cm^3g^{-1} and the pore diameter reduced from 3.77 to 3.64 nm for the Si/Al ratio of 50 to 7, respectively. ^{27}Al and ^{29}Si solid state NMR and IR spectroscopy results indicated that diminish in Si/Al ratio changed the structures, which led to generate of the strong Brønsted and Lewis acidic sites.

^{27}Al NMR confirmed the presence of tetrahedral, pentahedral and octahedral aluminium structures which 5-coordinate aluminium structure was observed only in Pt/HAlMSN-7. FTIR adsorbed pyridine results showed that the increasing in Si/Al ratio decreased the number of acid sites which led to decrease the catalytic activity towards cumene conversion.

Cumene conversion over these catalysts revealed an increase in cracking from Si/Al of 50 to 10 (from 84 to 97%) and decrease in Pt/HAlMSN with Si/Al of 7 (94%) due to the presence of pentahedral aluminium and/or inactive tetrahedral aluminium atoms. The mechanisms of dehydrogenation on Lewis acid sites is responsible for α-methylstyrene formation and dealkylation process produce propene, benzene, and toluene via a cracking on protonic acid sites through the Brønsted acidity.

The stability test showed that although the coke formation could gradually effect on the activity of these catalysts, the large amount of active surface area and pore size were still remained after 100 h of reaction.

The molar coefficient absorbance of Pt/HAlMSN samples was calculated using pyridine followed by water adsorption examined by FTIR spectroscopic which is a technique to measure the Brønsted and Lewis acid sites strength in the catalysts.

Acknowledgment

This work was supported by the Universiti Teknologi Malaysia under RUG Project No. 06H17. Our gratitude also goes to the Hitachi Scholarship Foundation, Japan for the Gas Chromatograph Instruments Grant.

References

1 J. S. Beck, J. C. Vartuli, W. J. Roth, M. E. Leonowicz, C. T. Kresge, K. D. Schmitt, C. T. W. Chu, D. H. Olson, E. W. Sheppard, S. B. Mc Cullen, J. B. Higgins and J. L. Schlenker, *J. Am. Chem. Soc.* 1992, **114**, 10834.

2 M. R. Sazegar, A. A. Jalil, S. Triwahyono, R. R. Mukti, M. Aziz, M. A. A. Aziz, N. H. N. Kamarudin and H. D. Setiabudi, *Chem. Eng. J.* 2014, **240**, 352.

3 J. H. Clark, D. J. Macquarrie and S. J. Tavener, *Dalton Trans.,* 2006, 4297.

4 M. A. A. Aziz, A. A. Jalil, S. Triwahyono, R. R. Mukti, Y. H. Taufiq-Yap and M. R. Sazegar, *Appl. Catal. B: Environmental,* 2014, **147**, 359.

5 K. O'Malley, A. Gil and T. Curtin, *Microporous Mesoporous Mater.,* 2012, **191**, 48.

6 N. H. N. Kamarudin, A. A. Jalil, S. Triwahyono, M. R. Sazegar, S. Hamdan, S. Baba and A. Ahmad, *RSC Adv.,* 2015, **5**, 30023.

7 H. D. Setiabudi, A. A. Jalil and S. Triwahyono, *J. Catal.,* 2012, **294**, 128.

8 N. H. N. Kamarudin, A. A. Jalil, S. Triwahyono, M. R. Sazegar, S. Hamdan, S. Baba and A. Ahmad, *RSC Adv.,* 2015, **5**, 30023.

9 S. K. Jana, H. Takahashi, M. Nakamura, M. Kaneko, R. Nishida, H. Shimizu, T. Kugita and S. Namba, *Appl. Catal. A: Gen.,* 2003, **245**, 33.

10 H. M. Moura and H. O. Pastore, *Dalton Trans.,* 2014, **43**, 10471.

11 S. Handjani, S. Dzwigaj, J. Blanchard, E. Marceau, J. M. Krafft and M. Che, *Top Catal.,* 2009, **52**, 334.

12 N. N. Ruslan, S. Triwahyono, A. A. Jalil, S. N. Timmiati and N. H. R. Annuar, *Appl. Catal. A: Gen.,* 2012, **413–414**, 176.

13 C. T. Kresge, M. E. Leonowiez, W. J. Roth and J. C. Vartuli, *US Pat.* 5,098,684, 1992.

14 L. Y. Chen, Z. Ping, G. K. Chuah, S. Jaenicke and G. Simon, *Microporous Mesoporous Mater.,* 1999, **27**, 231.

15 J. Liu, L. Zhang, Q. Yang and C. Li, *Microporous Mesoporous Mater.,* 2008, **116**, 330.

16 F. Subhan and B. S. Liu, *Chem. Eng. J.,* 2011, **178**, 69.

17 Y. Wang, N. Lang and A. Tuel, *Microporous Mesoporous Mater.,* 2006, **93**, 46.

18 X. W. Cheng, Q. P. He, J. Guo, H. Yan, H. Y. He and Y. C. Long, Microporous Mesoporous Mater., 2012, **149**, 10.

19 B. M. De Witte, P. J. Grobet and J. B. Uytterhoeven, *J. Phys. Chem.,* 1995, **99**, 6961.

20 P. Bhange, D. S. Bhange, S. Pradhan and V. Ramaswamy, *Appl. Catal. A: Gen.,* 2011, **400**, 176.

21 M. Bevilacqua, T. Montanari, E. Finocchio and G. Busca, *Catal. Today,* 2006, **116**, 132.

22 A. Jentys, N. H. Pham and H. Vinek, *J. Chem. Soc., Faraday Trans.,* 1996, **92**, 3287.

23 W. Daniell, U. Schubert, R. Glöckler, A. Meyer, K. Noweck and H. KnÖzinger, *Appl. Catal. A: Gen.*, 2000, **196**, 247.

24 T. N. Vu, J. van Gestel, C. Collet, J. P. Dath and J. C. Duchet, *J. Catal.,* 2005, **231**, 453.

25 P. Alexandru and J. T. William, *Ind. Eng. Chem. Res.,* 2003, **42**, 5988.

26 I. S. Pieta, M. Ishaq, R. P. K. Wells and J. A. Anderson, *Appl. Catal. A: Gen.,* 2010, **390**, 127.

27 T. Onfroy, G. Clet, and M. Houalla, *Micropor. Mesopor. Mater.,* 2005, **82**, 99.

28 C. A. Emeis, *J. Catal.*, 1993, **141**, 347.

29 D. J. Rosenberg, B. B. Baeza, T. J. Dines and J. A. Anderson, *J. Phys. Chem. B,* 2003, **107**, 6526.

30 D. J. Rosenberg and J. A. Anderson, *Catal. Lett.,* 2002, **83**, 59.

31 B. Wang, X. Wu, R. Ran, Z. Si, D. Weng, J. Mol. Catal. A: Chem. 361–362 (2012) 98–103.

32 R. Mokaya, W. Jones, Z. Luan, M. D. A. Klinowski and J. Klinowski, *Catal. Lett.,* 1996, **37**, 113.

33 Y. Kanda, T. Kobayashi, Y. Uemichi, S. Namba and M. Sugioka, *Appl. Catal. A: Gen.,* 2006, **308**, 111.

34 S. N. Timmiati, A. A. Jalil, S. Triwahyono, H. D. Setiabudi and N. H. R. Annuar, *Appl. Catal. A: Gen.,* 2013, **459**, 8.

35 S. M. Bradley and R. A. Kydd, *J. Catal.,* 1993, **141**, 239.

36 T. Mishra and K. Parida, *Appl. Catal. A: Gen.,* 1998, **174**, 91.

37 A. Corma, P. J. Miguel and A. V. Orchilles, *J. Catal.,* 1994, **145**, 58.

38 A. Corma and B. W. Wojciechowski, *Catal. Rev. Sci. Eng.,* 1982, **24**, 1.

39 N. H. R. Annuar, A. A. Jalil, S. Triwahyono, N. A. A. Fatah, L. P. The and C. R.. Mamat, *Appl. Catal. A: Gen.,* 2014, **475**, 487.

40 D. Trong On, S. M. J. Zaidi and S. Kaliaguine, *Micropor. Mesopor. Mater.,* 1998, **22**, 211.

41 R. Contreras, J. Ramirez, R. Cuevas-Garci, A. Gutierrez-Alejandre, P. Castillo-Villalon, G. Macias and I. Puente-Lee, *Catal. Today*, 2009, **148**, 49.

42 T. Kusakari, K. Tomishige and K. Fujimoto, *Appl. Catal. A: Gen.*, 2002, **224**, 219.

43 K. Hamaguchi and H. Hattori**,** Reaet. Kinet. Catal. Lett., 1997, **61**, 13.

44 M. A. A. Aziz, A. A. Jalil, S. Triwahyono and M. W. A. Saad, *Chem. Eng. J.,* 2015, **260**, 757.

Table of contents entry

Synthesizing Pt/HAlMSN with ratio of Si/Al=7-50 showed high activity in cumene hydrocracking due to the Brønsted and Lewis acid sites.